# 12 Effect of AC Ripple on VRLA Battery Performance

Scott D. Gerner and Tom E. Ruhlmann
Dynasty Division, C&D Technologies
900 E. Keefe Ave
Milwaukee, WI 53212

## INTRODUCTION

Superimposed AC ripple on lead-acid batteries used in float service has the potential to produce battery heating depending upon the AC magnitude and frequency. Battery service life is roughly halved the life for every 10°C increase in temperature. To date, few actual test results have been published to equate the magnitude of AC ripple with the resulting temperature rise and actual impact on service life. In this paper, we present actual VRLA product responses to AC ripple and discuss the potential impacts on life.

## BACKGROUND

A survey of product literature and technical papers shows limited published information of the effects of AC ripple[1-4]. A maximum 0.5% RMS ripple voltage ($V_{RMS}$) is specified in Dynasty product literature and is also a generally accepted industry guideline; however, it is the AC ripple current ($A_{RMS}$), which causes battery heating and reduced life. In this paper, we quantify the relationship between ripple current and voltage and their effects on battery performance. Within the industry, there has been a conscious effort to minimize the magnitude of AC ripple and increase the frequency to well beyond 60 Hz. The following tests were conducted at 60 Hz, being the lowest and worst case frequency typically encountered.

## TEST METHOD

### Batteries

Standard production Dynasty gelled and absorbent glass mat (AGM) Valve Regulated Lead Acid (VRLA) batteries were tested. All models are 12-volt, flat plate, recombinant designs. Models included the UPS12-95 (AGM, 33 AH at the 20 hour capacity), UPS12-270 (AGM, 75 AH) and the U131-A (gel, 31 AH). Each battery was equipped with mercury/mercury sulfate ($Hg/Hg_2SO_4$) reference electrodes to allow measurement of the positive and negative half-cell voltages. Thermocouples were mounted within the element, on the outer case side wall with insulated backing, to the negative terminal post and in ambient air.

### Test Equipment

A 60 Hz AC generator with an adjustable current output of 0-15 $A_{RMS}$ was constructed for experimental purposes. Batteries were placed on constant voltage float charge at 2.25 - 2.40 volts per cell using a Hewlett Packard DC power supply. An AC filter was also constructed and placed at the output of the DC power supply, in order to allow the power supply to maintain a consistent float voltage. Single 12-volt batteries were used for all testing. A 1 amp / 50 mV current shunt was used to measure the battery DC current acceptance; a 50 amp / 50 mV shunt was used to measure the AC current. Current, voltage and temperature data were collected at 10-minute intervals using a Fluke Hydra Data Bucket. AC waveforms (battery, cell and half-cell level) were measured and recorded using a Fluke 123 Scopemeter (20 MHz). Battery resistances were measured with an HP4338B milli-ohmmeter.

### Set Up

Testing started with the UPS12-270, then proceeded with the UPS12-95 and U131-A, in a progression of increasing battery resistance. All tests started with batteries at, or near 100% state of charge. Batteries were constant voltage float charged for a minimum of 24 hours at the test voltage with only the DC supply. AC ripple from the DC supply was negligible at less than 1 mV RMS across the battery. When the current acceptance had stabilized, the AC generator was turned on, typically to 100% maximum output for 24 to 48 hours, or until the internal temperature had stabilized. Tests were conducted at the laboratory ambient temperature of ~20-25°C, with the battery in open air, sitting on a bench top. Battery temperature was not controlled and allowed to fluctuate with the laboratory daily heating/cooling cycle. See Figure 1 for a schematic of the test layout.

## THEORY

### VRLA Battery Design

VRLA battery designs utilize the oxygen recombination cycle in order to minimize off gassing and water loss. By design, VRLA products need to be electrolyte starved to allow the oxygen evolved at the positive plate during float charge to easily pass through the open pores in the separator and react at the negative plate. The recombination of oxygen at the negative plate minimizes hydrogen evolution and the loss of water in the form of oxygen and hydrogen. However, the reduction in electrolyte volume in a VRLA product compared to that of a non-recombinant, flooded product make the VRLA batteries more sensitive to temperature, by reducing the battery's heat capacity and heat transfer coefficient. In addition, the recombination reaction is exothermic (heat generating), further enhancing temperature sensitivity and the phenomenon of thermal runaway [5].

### Temperature Effects on Life

A lead-acid battery's float service life is strongly dependent upon temperature, with life typically limited by positive grid corrosion. Like most chemical reactions, the corrosion rate doubles, or the life is cut in half for every 8-10°C increase in temperature. In addition to direct current and voltage battery heating effects, AC ripple current and voltage is also a concern as it can cause both mechanical (ohmic) and electrochemical (Faradaic) heating, dependent upon the frequency and magnitude.

### Voltage/Current Effects

A battery's charge/discharge voltage response is a function of the applied current. Figure 2 shows an equivalent battery circuit diagram. The mechanical components can be treated as a series of resistors, where the voltage drop through each component (terminal, strap lead, grids/paste, separator and electrolyte) follow Ohms law, $\Delta V=IR$. Their resistance accounts for the majority of $I^2R$ type heating. The typical resistive contribution of each component expressed as a percentage of the total battery resistance is shown in Figure 2. The electrochemical resistance, or polarization, is current dependent, but in a non-linear manner (Tafel curve). The equivalent circuit for each plate consists of a capacitor ($C_{Dbl}$, double layer capacitance) in parallel with two series resistors. The resistors account for electrochemical ($R_F$, Faradaic) and diffusion ($R_W$, Warburg) effects. The Warburg resistance term is typically shorted at frequencies > 10 Hz.

### AC Ripple

The positive and negative plate surfaces act as double layer capacitors. At high ripple frequencies, typically >333 Hz, only the double layer capacitor is charged and discharged. The high ripple frequency and double layer do not allow the plates to be charged and discharged, or cycled. In the intermediate frequency range from 1-333 Hz, the battery may be affected by AC ripple, dependent upon the battery design. At low frequencies, typically < 1 Hz, the ripple is slow enough to result in cycling, but the $A_{RMS}$ magnitude must also be considered.

AC voltage ripple ($V_{RMS}$) creates a corresponding current ripple ($A_{RMS}$). If the $A_{RMS}$ is high enough, the peak to peak cell voltage may vary around the nominal float voltage (2.25-2.30 V/cell) to such a degree that it will drop to a value lower than the open circuit voltage (~2.12-2.16 V/cell) and rise to an equal $\Delta V$ above the float voltage. The high $A_{RMS}$ effectively discharges and recharges the cell on each AC cycle. Increased gassing (dry out) and grid corrosion may occur when the cell voltage exceeds the nominal float voltage. Excessive cycling can lead to plate wear out. Cycling may also lead to a "walk-down" in capacity due to inefficiencies in the recharge process compared to the efficient discharge reaction. Even without cycling, $A_{RMS}$ still produces ohmic heating and an increase in the nominal float voltage.

Impedance spectroscopy can be used to develop a battery's frequency response and susceptibility to AC. Theoretical calculations of the battery's capacitance and RC time constant can be compared to the AC frequency to estimate the filtering capability of the double layer capacitor.

**Heat Balance**

In the simplest case, the heat input to a battery during steady state float operation is primarily due to resistance type heating:

(1) Heat Input, Watts = $I^2 \times R$

where I = float current in amps and R = battery resistance in ohms. In this case, resistance is almost solely due to ohmic rather than electrochemical resistance. Ohmic resistance can be measured directly with a milli-ohmmeter or calculated using the resistivity ($\rho$, ohms-cm), current path length (l, cm) and cross sectional area (A, $cm^2$) of each internal component ($\rho l/A$). Measured and calculated ohmic values are typically in good agreement, within $\pm$ 3%. The superimposed $A_{RMS}$ can be added to the DC value to calculate the $I^2R$ heating, adjusting equation 1 as follows, $(I_{A,RMS}+I_{DC})^2 \times R$.

At ambient temperatures of ~20-25°C, the current acceptance during float charge (2.25-2.30 V/cell) is typically on the order of 0.2-0.5 mA/AH (AH at the 20 hour rate). Due to the battery's relatively low internal resistance, typically on the order of milli-ohms/cell, $I^2R$ heating due to DC float current is negligible. In normal float voltage conditions, with minimal current input and gassing, the battery's internal resistance decreases for increasing temperature. As the ambient temperature or float voltage increase, the battery's current acceptance increases and therefore the temperature can rise due to $I^2R$ type heating.

Battery heat output is directly proportional to the product of its heat transfer coefficient (H, Watts/$meter^2$-°C), exposed surface area (A, $meter^2$) and the temperature differential versus ambient (T, °C), and can be expressed as:

(2) Heat Output, Watts = $H \times A \times (T_{BATTERY} - T_{AMBIENT})$

The heat transfer coefficient, is simply the rate a battery can move heat from internal components and reject it to the outside environment, and is dependent upon both battery and cabinet design. Battery orientation and spacing are important considerations in cabinet design to maximize heat output and minimize battery heating.

During steady state float conditions, the heat input and heat output balance and equations 1 and 2 can be set equal to each other and the resulting steady state battery temperature or temperature rise can be predicted by:

(3) $T_{BATTERY} - T_{AMBIENT} = (I^2 \times R) / (H \times A)$

The battery temperature is primarily dependent on the $A_{RMS}$ magnitude, regardless of the AC frequency.

## RESULTS AND DISCUSSION

**AC Ripple Voltage Response to Applied DC Float Voltage**

In the first series of tests, 13 $A_{RMS}$ at 60 Hz was forced into the battery while at an applied constant voltage float range of 2.25-2.40 volts/cell. The voltage response of a UPS12-270, yielding a peak to peak (p-p) voltage of 124 mV/battery or 44 $mV_{RMS}$ at 60 Hz (16.7 ms cycles) on float at 13.62 volts (2.27 V/c) is shown in Figure 3. With increasing applied float voltage up to 2.40 volts/cell, the peak to peak voltages did not change significantly, see Table 1. At 124 mV (p-p), the float voltage ranges from 13.56 to 13.68V, well above the open circuit voltage of 12.84V and within the specified float voltage window of 2.25-2.30 V/c. The ripple current is solely a plate surface, double layer capacitor phenomena, not causing true cycling.

Voltage ripple was also monitored at the cell and plate level, results are shown in Table 1. Although peak to peak voltages are the proper unit of measure for battery voltage effects, $mV_{RMS}$ and $A_{RMS}$ values are used for calculating heating and for ease of measurement ($mV_{RMS}$ x 1.414 = p-p voltage). At the cell level, the voltage ripple was uniform, averaging 7-8 $mV_{RMS}$, regardless of the applied float voltage. Using reference electrodes, positive and negative plate $mV_{RMS}$ were directly measured. With the UPS12-270 and other tests, the negative absorbed 65-75% of the total $mV_{RMS}$. For double layer capacitance effects, the voltage response is inversely proportional to the true BET paste surface area. Adding electrolyte to the recombinant system and to make it behave more like a "flooded" design, did not change the voltage response.

For reference and spec purposes, the term $V_{RMS}$% is used. This value is the ratio of measured $V_{RMS}$ to the applied float voltage. As shown in Table 1, $V_{RMS}$% is not significantly affected by float voltage. Note the significant difference (AC/DC ratio of ~300-600) between the magnitude of the AC and DC current. The step increase in DC acceptance at 2.25 V/c (pure DC to AC+DC) may be due to AC heating. The DC acceptance increase from 2.25 to 2.29 to 2.40 V/c is primarily due the applied voltage. No significant differences in temperature were noticed as the float voltage increased, as the AC current is the primary contributor to heating and was fixed at 13.2 $A_{RMS}$.

**Table 1 Average Cell and Plate Voltage Ripple vs. Applied Float Voltage, UPS12-270**

| | Pure DC | AC + DC | | |
|---|---|---|---|---|
| Applied Volts/cell | 2.25 | 2.25 | 2.29 | 2.40 |
| $A_{RMS}$ (Amps) | 0 | 13.2 | 13.2 | 13.2 |
| DC (Amps) | 0.020 | 0.021 | 0.030 | 0.046 |
| $mV_{RMS}$/cell | | 7.3 | 7.3 | 8.0 |
| $V_{RMS}$ % | | 0.32 | 0.32 | 0.33 |
| Positive $mV_{RMS}$ | | 2.5 | 2.0 | 2.1 |
| Negative $mV_{RMS}$ | | 4.8 | 5.3 | 5.9 |

### Cell Temperature Profiles

A temperature gradient exists within each cell and varies in response to the external ambient temperature and internal factors such as charge voltage, gassing, recombination and AC ripple. The battery temperature was not directly controlled, but instead was allowed to vary with the ambient temperature swings in the lab environment. The battery was outfitted with thermocouples to monitor the temperature gradient and its response. The ambient temperature was sensed ~12 inches above the battery in open air. The battery skin temperature was measured in direct contact with the side case wall in cell 3, at the mid-point of the case height, with the thermocouple tip insulated from behind. Internal temperatures were monitored in cell 3 with one thermocouple on the inside of the case wall opposite the outer one, another in contact with the lead strap connecting the negative plates and another buried ~2 inches deep within the center of the plate stack. The UPS12-270 plates are 6.0" high x 6.0" wide. Due to difficulties in inserting the thermocouple into the center of the AGM plate stack without damaging the battery or thermocouple, in subsequent tests, the temperature was sensed at the top of the plate stack.

During "pure" DC float at 2.27 V/c, with the current stabilized, the temperature gradient vs. time for a UPS12-270 for a 30 hour period is shown in Figure 4. Note how the plate center temperature lags the ambient temperature by the greatest margin, with the strap and case wall following in succession. This type of internal lagging profile is indicative of externally driven heating. For graphical legibility, only selected temperature profiles are shown; however, the inside case wall and terminal post temperatures also follow the expected pattern. The DC current acceptance is stable and extremely low, accounting for the ~0.5°F average internal - ambient temperature differential.

Once the 13 $A_{RMS}$ AC is applied, the temperature profiles quickly diverge as shown in Figure 5, taking about 7 hours to reach steady state. The internal temperature no longer lags the external, due to internal heating. The daily lab temperature cycling is still evident, but the plate top - ambient average differential is relatively constant at ~2.5 °F. Due to the failure of the plate stack thermocouple, the temperature was measured at the plate tops. The average difference between the plate top and internal plate stack is ~0.5 °F, so the true internal to ambient temperature differential averaged ~3.0 °F.

Temperature effects in a UPS12-95, with and without AC (13 $A_{RMS}$) are shown in Figure 6 and yield results similar to the UPS12-270 but with a 3.5 - 4.0°F inside-ambient temperature differential due to the UPS12-95's lower opposed plate surface area and higher resistance. Voltage ripple increased to 66 $mV_{RMS}$ or 0.48 $V_{RMS}$%. Cell and half-cell voltage ripple were corresponding higher, but uniform at 11 $\pm$ 0.5 $mV_{RMS}$/cell (8 $mV_{RMS}$ negative/ 3 $mV_{RMS}$ positive).

Temperature effects in the U131-A gelled battery, with and without AC (14.6 $A_{RMS}$) follow a similar trend with a 4.5°F inside-ambient temperature differential due to this product's even lower opposed plate surface area and higher resistance due to gelled vs. AGM construction. Voltage ripple increased to 150$mV_{RMS}$ or 1.1 $V_{RMS}$%. Cell and half-cell voltage ripple were corresponding higher, but uniform at 25 $\pm$ 2 $mV_{RMS}$/cell (18 $mV_{RMS}$ negative/ 7 $mV_{RMS}$ positive). Even at this high ripple current, the $mV_{RMS}$/cell is not high enough to cause charge/discharge type cycling.

### Resistive Heating

The prior tests were conducted with the maximum AC output in order to obtain the maximum temperature rise for each model. For additional comparative purposes, the temperature and voltage response was studied at ~6, 9, 12 and 14.6 $A_{RMS}$ using the U131-A. The temperature rise (internal – ambient) is plotted against AC current in Figure 7 and shows the temperature to increase in proportion to the square of the current. Plugging in the heat transfer coefficient, surface area and resistance terms into equation 3, the predicted vs. actual observed temperature rise show very good agreement. At 60 Hz AC, the temperature rise is primarily due to $I^2R$ type heating. Even at full output, the peak to peak voltage deviation around the mean float voltage was not large enough to cause charge/discharge type cycling and further heating.

The heat transfer coefficient and surface area terms are in the denominator of equation 3. As both terms decrease in value, the temperature rise increases. Flooded batteries have higher heat transfer coefficients than gel which are higher than AGM designs[5]. The increased heat transfer helps to "cool" the battery primarily due to the conductive path between the electrolyte surrounding the internal battery components and the case wall. Although these tests were conducted with single batteries on a ventilated bench top, surface area, which can be varied by battery orientation and spacing, can also affect temperature rise.

Product float life is strongly dependent upon battery temperature, so the maximum allowable ripple current will directly affect service life. Using the rule of thumb that the service life is halved for every 10°C (18°F) increase in temperature, the reduction in life vs. $A_{RMS}$ is plotted in Figure 7 for the U131-A. Assuming 100% life with pure DC, float life will be reduced by 5% at ~8 $A_{RMS}$ due to $I^2R$ type heating and by 10% at ~11 $A_{RMS}$.

### Voltage Ripple, $V_{RMS}$

The $V_{RMS}$% response varies with $A_{RMS}$, but is also dependent upon battery design. Correlation of $V_{RMS}$ to battery heating is less direct, results for all 3 test models are shown in Figure 8. At 0.5% $V_{RMS}$, the temperature rise ranged from 1.2-3.6°F for the U131-A and UPS12-95 (5-13% life reduction). While the models are rated at 31 and 33AH, the AGM product's larger opposed plate surface area results in significantly reduced $V_{RMS}$, 0.5 vs. 1.0% at 13 $A_{RMS}$.

Battery resistance vs. 20 hour AH capacity is plotted in Figure 9. Resistance increases as the product's AH rating decreases or for a given AH capacity, as the plate count (opposed plate surface area) decreases. As defined in equation 3, higher resistance leads to proportional increases in battery temperature due to $I^2R$ heating. The use of the ratio $A_{RMS}$/AH to broadly define AC ripple guidelines can be misleading as heating is due to the square of the current and the variable relationship between AH and resistance.

### Conclusions

AC ripple causes ohmic ($I^2R$) heating that is a major contributor to battery heating. By minimizing AC ripple and with careful attention to battery cabinet layout, product float life can be maximized. Directly measuring battery temperature provides the best means to monitor the effects of AC ripple.

### Acknowledgements

This paper was made possible in part through the able assistance of Steve Jensen and Chad Ganshow, who assembled the equipment and conducted the tests. I also thank Wen-Hong Kao for his insightful direction and comments.

### References

1. S. Okazaki, *"Influence of superimposed alternating current on capacity and cycle life for lead-acid batteries"*, Journal of Applied Electrochemistry 16 (1986) pgs 894-898.
2. D. Wilson, *"The Measurement of Ripple Current in Battery Plants"*, Paper 18-1, Proceedings of the Tenth INTELEC, 1988.
3. W. Rutledge, *"Service Life Limitations of Flooded Lead Acid Batteries in UPS Service"*, Paper 18-2, Proceedings of the Tenth INTELEC, 1988.
4. S. Misra, *"Stationary Battery Design and Usage and Its Impact On Life"*, Paper 12-6, Proceedings of the Twelfth INTELEC, 1990.
5. S. Gerner, G. Brilmyer, D. Bornemann, *"Thermal Management of Valve Regulated Lead-Acid Batteries, A Comparison of Gelled vs. Absorbed Electrolyte Technologies"*, Paper 9-3, Proceedings of the Twelfth INTELEC, 1990.

**Figure 1 AC Ripple Test Layout**

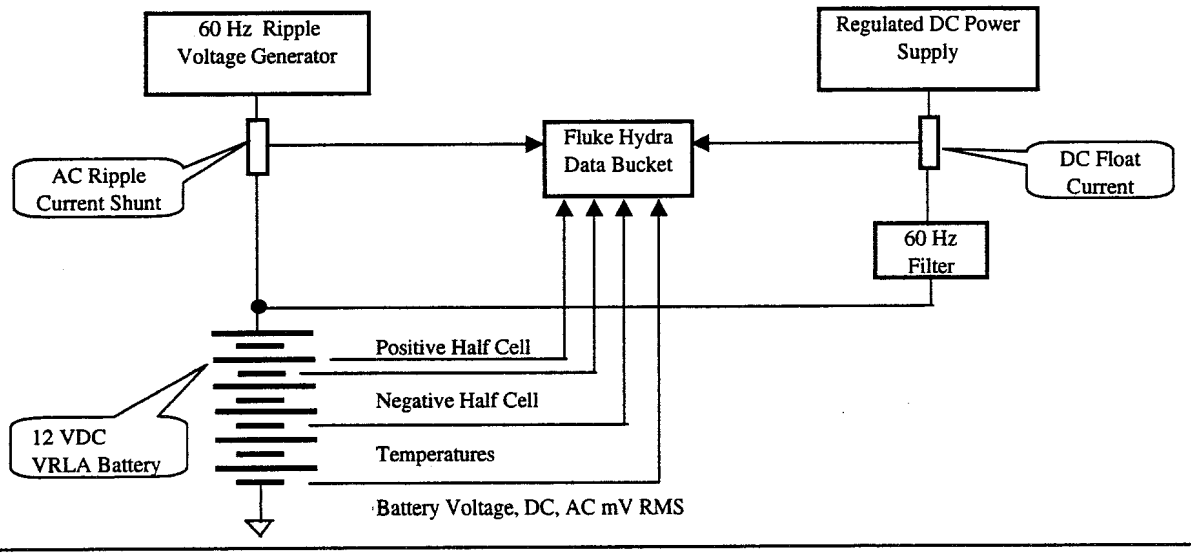


**Figure 2 Battery Equivalent Circuit**

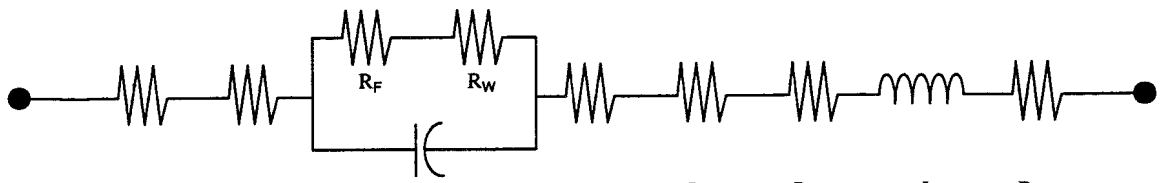


| Component | $R_{Term}$ | $R_{Strap}$ | $R_{Grid}$ | $R_{Sep}$ | $R_{Elyte}$ | L | $R_{Weld}$ |
|---|---|---|---|---|---|---|---|
| Resistive % | 12% | 25% | 40% | 1% | 15% | | 7% |

**Figure 3 Induced AC Voltage Ripple, UPS12-270 Floating at 13.62 Volts**

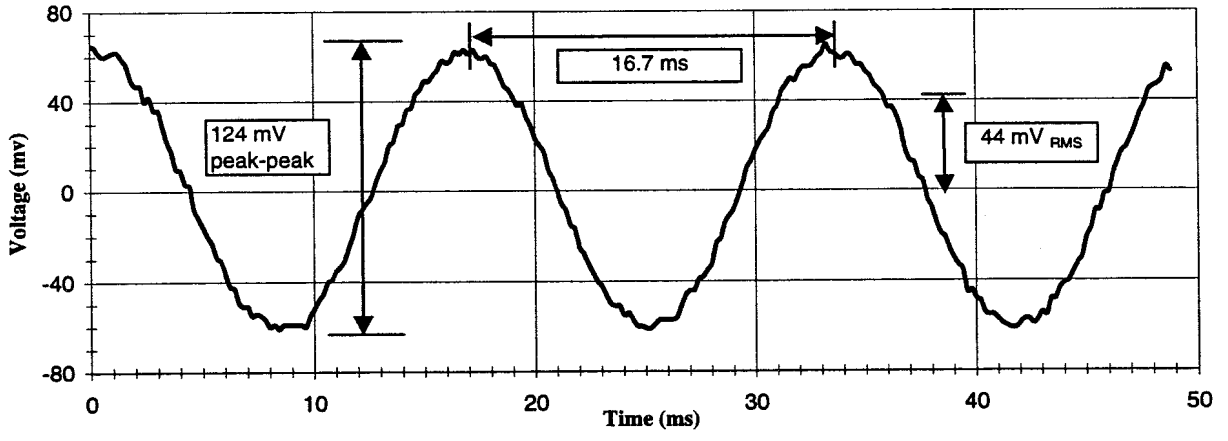

Figure 4 UPS12-270 Temperature by Position, DC Float

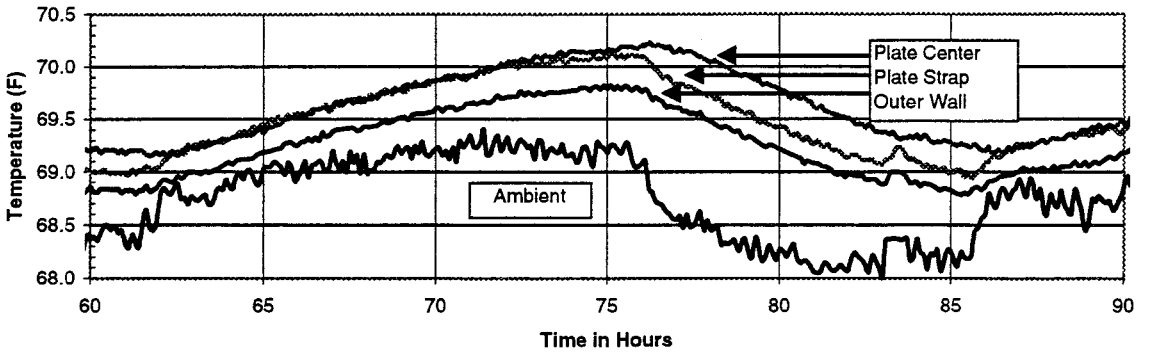


Figure 5 UPS12-270 Temperature by Position, AC Ripple

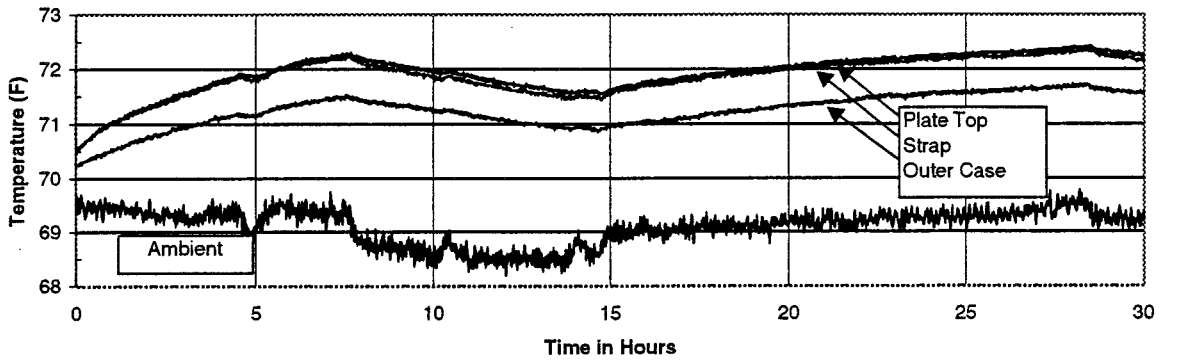


Figure 6 UPS12-95 Temperature with AC Ripple Off / On

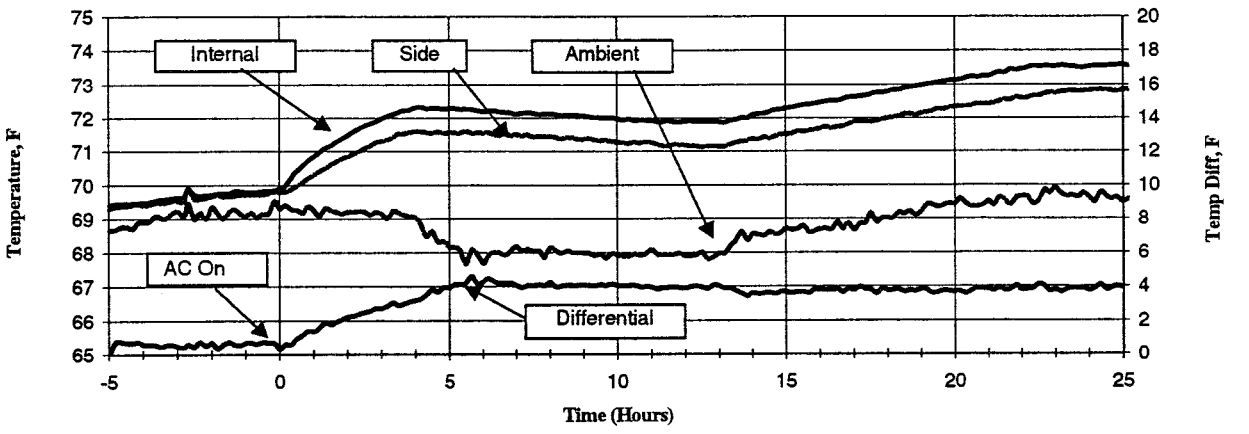

**Figure 7 Temperature Rise, Relative Life vs. AC Amps U131-B**

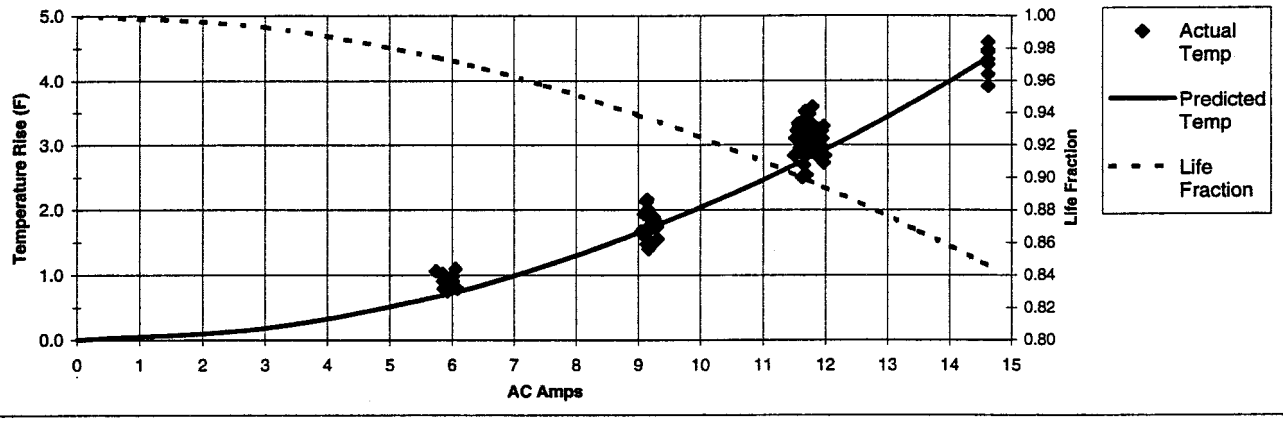


**Figure 8 Temperature Rise vs. AC Voltage Ripple $V_{RMS}$%**

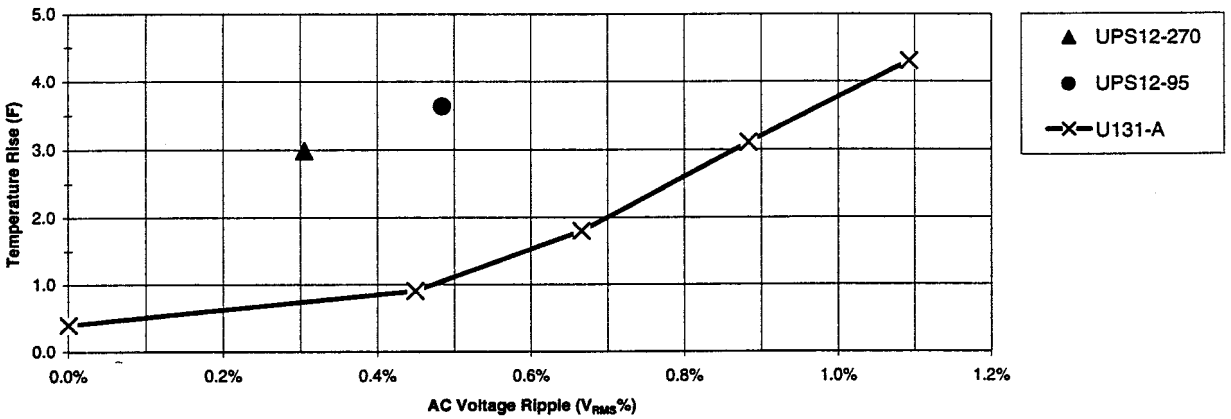


**Figure 9 Battery Resistance vs 20 Hour AH Capacity**